

# Therapeutic potential of sulforaphane: modulation of NRF2-mediated PI3/AKT/mTOR pathway in oral fibrosis

Potencial terapêutico do sulforafano: modulação do NRF-2 mediado o pela via PI3/AKT/mTOR na fibrose oral

Pooja Narain ADTANI<sup>1</sup> , Rajasekaran SUBBARAYAN<sup>2</sup> , Rupendra SHRESTHA<sup>3</sup> , Walid ELSAYED<sup>1</sup> 

1 - Gulf Medical University, College of Dentistry, Department of Basic Medical and Dental Sciences. Ajman, United Arab Emirates.

2 - Chettinad Academy of Research and Education, Chettinad Hospital and Research Institute, Faculty of Allied Health Sciences, Center for Advanced Biotherapeutics and Regenerative Medicine. Chennai, India.

3 - Anka Analytica, Research and Collaboration. Melbourne, Victoria, Australia.

**How to cite:** Adtani PN, Subbarayan R, Shrestha R, Elsayed W. Therapeutic potential of sulforaphane: modulation of NRF2-mediated PI3/AKT/mTOR pathway in oral fibrosis. *Braz Dent Sci.* 2024;27(1):e4172. <https://doi.org/10.4322/bds.2024.e4172>

## ABSTRACT

Oral Submucous Fibrosis is a potentially malignant disorder caused by habitual areca nut chewing, which contributes to the dispersion of active alkaloids into subepithelial tissues, stimulating excessive extracellular matrix deposition. Various treatment modalities are available; however, their efficacy in inhibiting fibrosis progression remains limited. Sulforaphane (SFN), an isothiocyanate found abundantly in cruciferous plants, is known to have effective antifibrotic properties. **Objective:** The present study investigated the antifibrotic effect of SFN via phosphatidylinositol 3 kinase (PI3K), Serine/Threonine Kinase 1 (AKT-1), mammalian target of rapamycin (mTOR) pathway in arecoline (AER) induced fibrosis in human gingival fibroblasts [HGFs]. **Material and Methods:** MTT assay determined the half-maximal inhibitory concentration of AER and SFN at 24h in the HGF cell line. Expression levels of transforming growth factor  $\beta$ 1 (TGF $\beta$ 1), collagen type 1 alpha 2 (COL1A2), hydroxyproline (HYP), PI3, AKT, mTOR, and nuclear factor erythroid 2-related factor 2 (NRF2) were assessed post-AER and SFN treatment using qPCR and western blot analysis. **Results:** The findings of the study revealed that AER elicited a stimulatory effect, upregulating TGF $\beta$ 1, COL1A2, HYP, PI3K, AKT, and mTOR and downregulating NRF2 expression. Conversely, SFN treatment significantly upregulated NRF2, inhibiting TGF $\beta$ 1 mediated PI3/AKT/mTOR pathway. **Conclusion:** These observations suggest that SFN can be used as a promising synergistic antifibrotic agent to combat fibrogenesis via the non-Smad pathway.

## KEYWORDS

Arecoline; NRF2; Oral submucous fibrosis; PI3/AKT/mTOR; Sulforaphane.

## RESUMO

Fibrose submucosa oral é uma desordem potencialmente maligna causada pelo hábito de mascar a noz da areca, o que contribui para a dispersão de alcalóides ativos nos tecidos subepiteliais, estimulando a deposição excessiva de matriz extracelular. Há várias modalidades terapêuticas, no entanto, com eficácia limitada no controle da progressão da fibrose. O sulforafano (SFN), isotiocianato encontrado abundantemente em plantas crucíferas, é conhecido por suas propriedades antifibróticas. **Objetivo:** Investigar os efeitos antifibróticos do SFN na via fosfatidilinositol3-quinase (PI3K), via quinase serina/treonina 1 (AKT-1), via do alvo da rapamicina em mamíferos (mTOR), na fibrose induzida por arecolina (AER) em fibroblastos gengivais de humanos (HGFs). **Material e Métodos:** A meia concentração inibitória mínima de AER e SFN em 24 horas nas células HGFs foi determinada por MTT. Os níveis de expressão de  $\beta$ 1 (TGF $\beta$ 1), colágeno tipo 1 alfa 2 (COL1A2), hidroxiprolina (HYP), PI3K, AKT, mTOR, fator nuclear eritroide 2 relacionado ao fator 2 (NRF2) foram analisados após tratamento com ERA e SFN através de qPCR e western blot. **Resultados:** O ERA apresentou efeito estimulatório aumentando a expressão de TGF $\beta$ 1, COL1A2, HYP, PI3K, AKT e mTOR e diminuindo a expressão de NRF2. Por outro lado, tratamento

com SFN aumentou significativamente a expressão de NRF2, inibindo a liberação de TGF $\beta$ 1 mediada pela via PI3/AKT/mTOR. **Conclusão:** Esses achados sugerem que o SFN pode ser um agente antifibrótico promissor no combate à fibrogênese decorrente da via não-Smad.

## PALAVRAS-CHAVE

Arecolina; NRF2; Fibrose submucosa oral; PI3/AKT/mTOR; Sulforafano.

## INTRODUCTION

Oral submucous fibrosis (OSF) is a chronic, progressive, and insidious collagen metabolic disorder that affects several parts of the oral cavity [1]. According to the World Health Organization (WHO) report in 2022, OSF has a global prevalence of 4.96%, with most cases in Southeast Asian countries such as India, Pakistan, Bangladesh, China, Taiwan, and Vietnam [2]. OSF has a multifactorial etiopathogenesis, such as genetic predisposition, autoimmunity, and vitamin deficiency, but the primary causative agent is arecanut or betelnut chewing [3]. One of the essential constituents of the arecanut fruit is the presence of an alkaloid arecoline (AER) which is hydrolyzed to arecaidine on reacting with lime. Both AER and arecaidine are carcinogenic and mutagenic, contributing to the malignant transformation of OSF to Oral Squamous Cell Carcinoma (OSCC) [1,4,5]. OSFs worldwide malignant transformation rate is estimated to be 1.2% to 23% and is classified as a potentially malignant disorder [6,7].

Several *in vitro* and clinical studies have reported AER-induced upregulation of transforming growth factor-beta 1 (TGF $\beta$ 1)/Smad signaling, collagen type 1 alpha 2 (COL1A2), collagen type 3 alpha 1 (COL3A1), beta fibroblast growth factor (bFGF), connective tissue growth factor (CTGF), alpha-smooth muscle actin ( $\alpha$ SMA), reactive oxygen species, tumor necrosis factor-alpha (TNF $\alpha$ ), matrix metalloproteinases, and downregulation of tissue inhibitors of metalloproteinases [6,8-10]. A few studies have also demonstrated the inductive effect of AER on HepG2 cells, promoting proliferation and migration of cells through the activation of the phosphoinositide 3-kinase/ mammalian target of rapamycin (PI3/AKT/mTOR) pathway [11].

The PI3/AKT/mTOR has also been explored in fibrotic conditions such as idiopathic pulmonary

fibrosis and liver fibrosis [12,13]. PI3/AKT/mTOR is an important intracellular signaling transduction pathway for cell survival, proliferation, apoptosis, and autophagy. Autophagy is a fascinating cellular process that enables cells to withstand various stresses and rid themselves of detrimental components [14]. Furthermore, inhibition of the mTOR signaling pathway is associated with the induction of autophagy primarily modulated by a master transcription factor called NF-E2-related Factor 2 (NRF2) [14-16].

The existing treatment modalities for OSF only provide temporary symptomatic relief as recurrence of the fibrotic bands is a common side effect observed after surgical interventions, highlighting the need for an effective intervention [17,18]. Therefore, developing antifibrotic approaches to attenuate oral fibrosis becomes a vital objective to prevent the malignant transformation of OSF. Sulforaphane (SFN) is a sulfur-containing isothiocyanate found abundantly in cruciferous vegetables such as cabbage, brussels sprouts, and broccoli. Several studies have reported SFN as a chemo-preventive agent functioning via NRF2-dependent induction of phase II detoxifying enzymes. Recent investigations suggest that the chemo-preventive effect of SFN is mediated through various mechanisms; for example, in breast and prostate cancer cell lines, it suppresses mTOR activity and induces autophagy. It is also known to cause cell cycle arrest, promote apoptosis, and inhibit angiogenesis and metastasis [19-21]. Additionally, SFN has demonstrated promising antifibrotic activity in renal fibrosis and pulmonary fibrosis in an NRF 2-dependent manner [22,23]. However, the potential effects of SFN in OSF and its impact on the profibrotic TGF $\beta$ 1 mediated PI3/AKT/mTOR pathway have not yet been assessed. Therefore, our study investigated the antifibrotic effect of SFN treatment in attenuating arecoline-induced fibrosis in human gingival fibroblasts [HGFs] via the PI3/AKT/mTOR pathway.

## MATERIAL AND METHODS

### Chemicals and consumables

All the cell culture plasticware and chemicals were purchased from Thermofisher Scientific, Mumbai, India, and Lonza, Basel, Switzerland. The kits were purchased from Sigma Aldrich, Missouri, USA. qPCR products, Verso cDNA Synthesis Kit from Thermofisher Scientific, Mumbai, India, and primers were purchased from Eurofins, Bangalore, India. Chemicals and materials for protein analysis were procured from Bio-Rad, CA, USA. All antibodies were purchased from Abcam, (Cambridge, UK, and Cell Signaling, Massachusetts, USA. D, L-Sulforaphane (CAS number – 4478937) and Arecoline hydrobromide (CAS number – 300083) were purchased from Sigma Aldrich, Missouri, USA.

### Human gingival fibroblast cell culture

Primary Gingival Fibroblast Human adult cells (HGF) were obtained from the American Type Culture Collection (ATCC - PCS-201-018). Cell suspensions were centrifuged at 1000 g for 5 min at 37°C; the obtained pellet was resuspended in complete media and seeded in 6 well plates containing complete media. HGFs were distributed evenly into a T75 flask in complete Dulbecco's Modified Eagle Medium (DMEM) Low Glucose (Lonza) supplemented with 10% Fetal Bovine Serum (Invitrogen), 100 U/mL penicillin, 100 µg/mL streptomycin, 100 µg/mL amphotericin B, 2 mM L-Glutamine and cultured at 37°C, 5% CO<sub>2</sub> in humidified tissue culture incubator. Growth media was changed every third day. The plastic adherent confluent cells were passaged with 0.05% trypsin containing 1mM Ethylenediaminetetraacetic Acid (EDTA) [24]. Cells from the 5<sup>th</sup>-6<sup>th</sup> passages were used for the experiments.

### Cell viability and proliferation assay

MTT (3-(4, 5-dimethyl thiazol-2yl)-2, 5-diphenyl tetrazolium bromide) assay was performed to determine the viability and cell proliferation rate of HGFs by colorimetric estimation [25,26]. Cultured HGFs were treated with various concentrations of SFN (1µM, 5µM, 10µM, 25µM, 50µM, 80µM, 100µM), and AER (0.0025 µg/mL, 0.25 µg/mL, 2.5 µg/mL, 25 µg/mL, 50 µg/mL, 100µg/mL) for 24h and 48h respectively [8,27]. SFN was dissolved

in 1X phosphate buffered saline and AER in dimethyl sulfoxide (DMSO). Next, 20µL of the MTT solution was thoroughly mixed in each well. The supernatants were aspirated after 4h of incubation, and 100 µL of DMSO was added to each well to dissolve the residue. Cell viability was estimated by measuring the absorbance at 570 nm in the IQuant ELISA plate reader, Vermont, USA. The cell viability percentage was determined by analyzing the absorbance ratio of cell cultures treated with SFN and AER. Cell viability expressed as a percentage of the control is determined by multiplying the untreated control by 100. After repeated SFN and AER dilutions, 50% cell death was used to calculate the cytotoxicity (IC<sub>50</sub>) ratio.

### Immuno-cytochemistry analysis of vimentin and TGFβ1

HGFs were cultured and induced with AER. After induction, HGFs were treated with SFN for 24h and fixed with 10% formalin for 30 min and ice-cold methanol for 20 min to promote permeabilization. Immunofluorescence staining was performed for anti-vimentin (Abcam – ab137321) to confirm the phenotypic properties of fibroblasts. 4',6-diamidino-2-phenylindole (DAPI) staining was performed to counterstain the nucleus. Images were captured at 20X magnification. Further, immunostaining was performed for anti-TGFβ1 (Abcam - ab9758) and secondary antibody (Goat anti-Rabbit IgG Alexa Fluor 488 (A32731) along with DAPI to confirm the fibrotic properties. Six different regions on the coverslip were focused, and images were recorded at 40X magnification. The fluorescence intensity was estimated using FIJI software, and the expression pattern of TGFβ1 was quantified (Arbitrary Units).

### Hydroxyproline estimation by colorimetric method

For hydroxyproline (HYP) estimation, cells were scraped out with 100 µL of water post 24h SFN treatment and transferred to a pressure-tight polypropylene vial with a poly tetrafluoro ethylene lined cap as per the manufacturer's protocol (Sigma-Aldrich, Cat no MAK008). 100 µL of concentrated hydrochloric acid (HCl, ~12 M) was added and capped tightly, followed by hydrolyses at 120°C for 3h. The contents were mixed and centrifuged at 10,000 rpm for 3 min, of which 10 - 50 µL of supernatant was

transferred to a 96-well plate. HYP in the sample was detected using a multiple spectrometer (Bio-Rad, Hercules, CA, USA) at 560 nm.

### RNA extraction and Quantitative Polymerase Chain Reaction (qPCR) analysis

#### RNA Isolation

According to the manufacturer's protocol, the TRIzol® method was used to extract total RNA of cell after 24h post SFN treatments.

#### Synthesis of Complementary DNA (cDNA)

Following the instructions provided by the manufacturer, the PrimeScript RT Master Mix (Takara Bio, Kusatsu, Japan) was utilized for cDNA synthesis. For each cDNA synthesis, 1 µg RNA was combined with 4 µL of 5X PrimeScript RT Master Mix and diluted to a final volume of 20 µL using RNase-free ddH<sub>2</sub>O from Takara Bio. A reverse transcription step of 15 min at 37°C, followed by a 5 s inactivation step at 85°C, and a holding temperature at 4°C were set on the Thermocycler T100 (Bio-Rad Laboratories, Hercules, CA, USA). The cDNA samples were promptly stored at -20°C. Experiment was conducted (qPCR) using power SYBR Green Master Mix to verify the amplification from the cDNA templates on a Quanta Studio 7 flex. An evaluation of the assay specificity for each gene of interest was conducted through melting curve analysis. A singular peak in the analysis indicates primer specificity. The present study investigated the genes related to fibrosis and receptor specific for SFN; TGFβ1, COL1A2, P13K, AKT, mTOR, and NRF2 in all the experimental samples. All reactions were performed in triplicates. Primers were designed using previously reported methods [28]. The primer pair specificity was confirmed using the Primer-Blast tool and

purchased from Eurofins Scientific, India. The primer sequences and accession numbers are listed in Table I. The protocol for RNA isolation, cDNA retro-transcription and amplification was standardized by the authors [28].

#### Western blot analysis

HGFs were subjected to 25 µg/mL of AER to induce a fibrotic condition [9] following which the cells received SFN treatment at a concentration of 10 µM. After 24h treatment, the proteins were extracted using RIPA Cell Lysis Buffer and carefully stored on ice for 30 min. The lysates were centrifuged at a speed of 12,000 g at a temperature of 4°C for 10 min. Later, the resulting liquid was carefully transferred to a new tube. Using the bicinchoninic acid (BCA) method, protein samples of 40 µg/lane were separated using SDS-PAGE and transferred into polyvinylidene fluoride membranes. A solution containing 10% bovine serum albumin (BSA) was utilized to block the membranes for one hour at room temperature. Next, the membranes were exposed to TGFβ1 (Abcam - ab9758), NRF2 (Abcam - ab62352), p-mTOR (Abcam - ab109268), mTOR (Abcam - ab137133), and β-Actin (Abcam - ab8226) antibodies. Then, the membranes were washed thrice and probed with secondary antibodies (Goat anti-Rabbit IgG Alexa Fluor 488 (A32731)). The detection was performed using enhanced chemiluminescence reagents from Pierce, Rockford, IL, USA. The intensities of the generated bands were measured using ImageJ software.

#### Statistical analysis

The assessed values are the mean ± standard error of the experimental samples, which include the control, AER treated, and AER with SFN treated, with n (3) biological triplicates. Statistical

**Table I** - Primer sequences and accession numbers.

Human Specific Gene	Forward Sequence	Reverse Sequence	Accession N°
TGFβ1	TACCTGAACCCGTGTTGCTCTC	GTTGCTGAGGTATCGCCAGGAA	NM 000660
COL1A2	CCTGGTGCTAAGGAGAAAGAGG	ATCACCACGACTTCCAGCAGGA	NM 000089
PI3K	GAAGCACCTGAATAGGCAAGTCG	GAGCATCCATGAAATCTGGTCGC	NM 006218
mTOR	AGCATCGGATGCTTAGGAGTGG	CAGCCAGTCATCTTTGGAGACC	NM 004958
AKT	TGGACTACCTGCACTCGGAGAA	GTGCCGAAAAGGTCTTCATGG	NM 005163
NRF2	CACATCCAGTCAGAAACAGTGG	GGAATGCTCTCGCCAAAAGCTG	NM 006164
TBP	TGTATCCACAGTGAATCTTGTTG	GGTTCGTGGCTCTCTTATCCTC	NM 003194

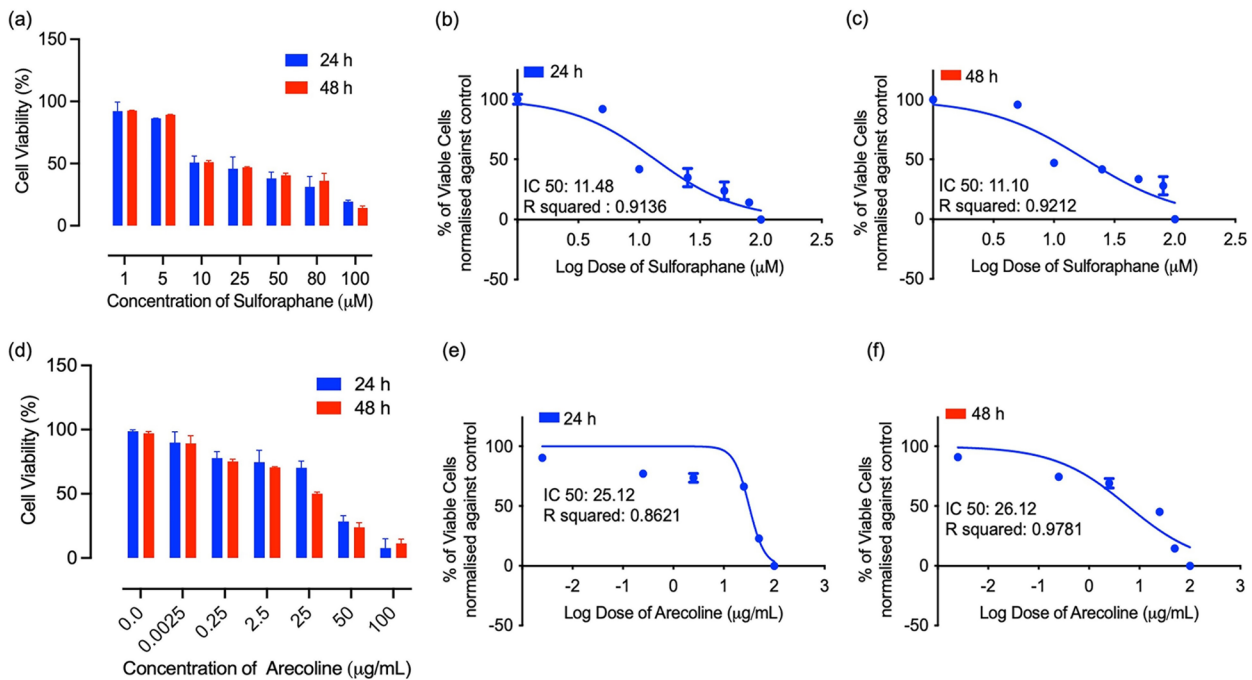


**Figure 1** - Graphical representation of cytotoxic effects of Sulforaphane (SFN) and Arecoline (AER) on Human Gingival Fibroblast (HGF) cells on 24h and 48h treatment. (a) Percentage of cell viability on treatment with different concentrations of SFN; (b) Half maximal inhibitory (IC<sub>50</sub>) for SFN was determined as 11.48  $\mu$ M at 24h; (c) Half maximal inhibitory (IC<sub>50</sub>) for SFN was determined as 11.10  $\mu$ M at 48h; (e) Half maximal inhibitory (IC<sub>50</sub>) for AER was determined as 25  $\mu$ g/mL at 24h; (f) Half maximal inhibitory (IC<sub>50</sub>) for AER was determined as 26.12  $\mu$ g/mL at 48h. IC<sub>50</sub> concentrations observed at 24h for SFN and AER were used for the study.

analysis was conducted using One-way ANOVA and a Bonferroni post hoc multiple comparison test, which provided a 95% confidence level. Using Graph Pad Prism 10.0, the intervals  $**p = <0.001$  and  $*p = 0.05$  were determined.

## RESULTS

### Cytotoxic effects of SFN and AER on HGFs

The initial findings of SFN and AER on HGFs showed that the level of cytotoxicity increased in a dose-dependent manner. Based on the MTT assay, it was observed that over 50% of the cells remained viable after 24h of incubation with SFN and AER, as shown in (Figures 1a and 1d). The results obtained were satisfactory. With increasing doses of as high as 100  $\mu$ M of SFN and 100  $\mu$ g/mL of AER per culture (Figures 1a and 1d), HGFs showed significantly reduced cell growth compared with the minimal concentration of SFN (1  $\mu$ M) and AER (0.0025  $\mu$ g/mL). Based on the data obtained from Figures 1a-f, it was determined that SFN had an inhibitory effect on cell growth of HGFs at a concentration 11.48  $\mu$ M, while AER exhibited the same effect at a concentration of 25  $\mu$ g/mL. To calibrate the experiment, a concentration of

10  $\mu$ M of SFN was utilized for the subsequent procedures.

### Immunofluorescence analysis of HGFs using TGF $\beta$ 1 and vimentin staining

Immunofluorescence staining with vimentin confirmed the spindle-shaped fibroblastic morphology and the mesenchymal origin of HGFs [29]. The nucleus of the cells was stained with DAPI (Figure 2a). Induction of AER in HGFs showed a significant increase in TGF $\beta$ 1 expression. However, after 24h of SFN treatment, a substantial reduction in TGF $\beta$ 1 expression was observed (Figure 2b). Furthermore, fluorescent intensity was quantified at a minimum of 6 fields of 10X magnification, corroborating with the captured image in Figure 2c.

### Effect of SFN on Hydroxyproline levels in AER-treated HGFs

We also confirmed the soluble collagen deposition by measuring the hydroxyproline (HYP) levels. The induced group (AER) showed significantly increased expression compared to the control. Interestingly, SFN treatment significantly reduced and regulated the development of fibrosis induced in the HGF cell model (Figure 2d).

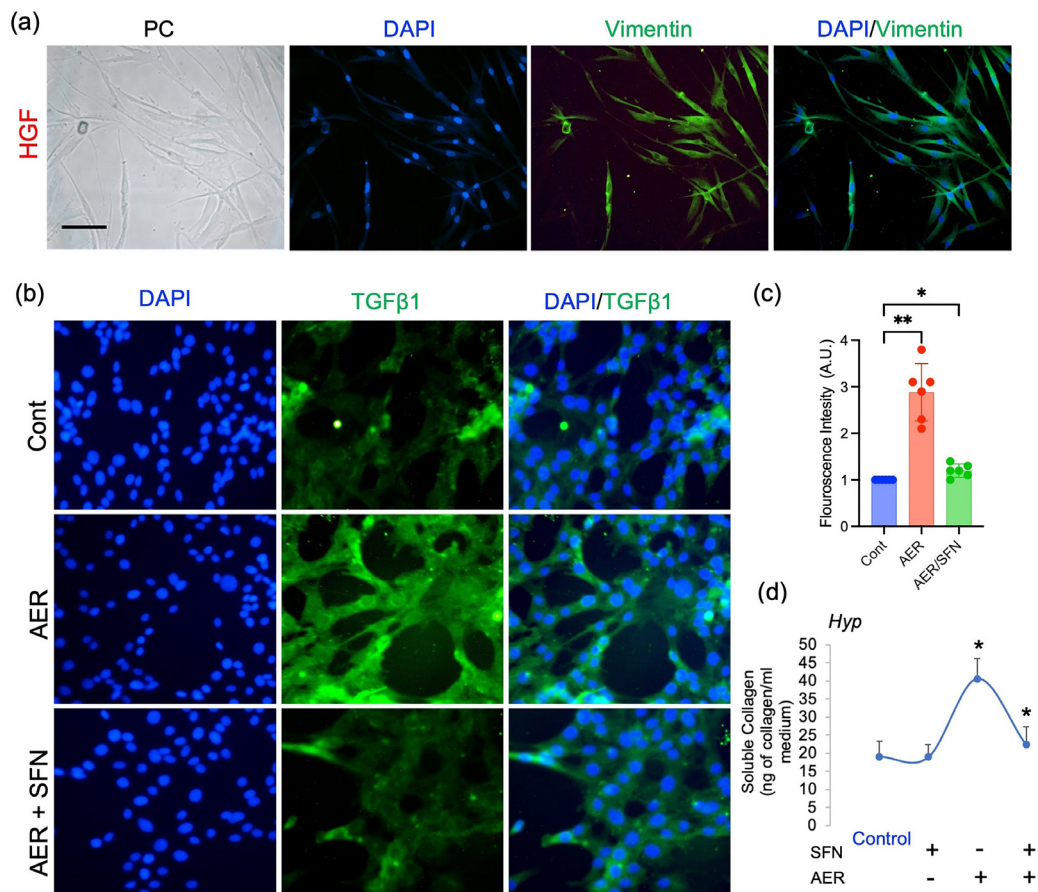


**Figure 2** - Immunofluorescence staining of Human Gingival Fibroblasts (HGFs) (a) [Left to right in the panel] - Phase contrast image, nucleus stained with DAPI, vimentin staining confirming the mesenchymal origin, and merged image (DAPI/Vimentin) (b) Comparison between control, AER treated, and AER and SFN treated group on staining with TGFβ1 and DAPI; (c) Graphical representation of fluorescent intensity quantification of a minimum 6 field of 10X magnification; (d) Graphic representation of hydroxyproline estimation on AER treatment and post-SFN treatment. \*\* $p < 0.01$ , \* $p < 0.05$

### Effect of SFN on TGFβ1 mediated PI3/AKT/mTOR

The mRNA analysis showed that the expression of crucial fibrotic markers (TGFβ1 and COL1A2) significantly increased in AER-treated cells compared to the control. On SFN treatment, a significant downregulation of the fibrotic markers was observed (Figures 3a and 3b). P13K, AKT, and mTOR expression on AER induction (25 μg/mL) significantly increased compared to the control group (Figures 3c, 3d and 3e). However, SFN (10 μM) treatment significantly reduced fibrosis in the induced HGF cells. In addition, our study results demonstrated that the expression levels of NRF2, an SFN-specific binding protein, were significantly reduced after AER induction. On the contrary, SFN treatment significantly upregulated NRF2 levels and confirmed that the antifibrotic effect of SFN is mediated via NRF2 (Figure 3f). The gene fold changes were calculated using  $\Delta\Delta C_t$ , and all

gene expressions were normalized with TBP. The illustration of gene expression represents a heat map, which elucidates the gene cluster orientation of the targeted gene (Figure 3g).

Furthermore, the protein analysis confirmed that the functional aspects of SFN treatment significantly reduced TGFβ1 and increased NRF2 expression following AER induction (Figure 4a). SFN treatment significantly reduced mTOR levels in the AER-induced HGFs (Figure 4c). Relative units were calculated from the densitometry value and normalized with β-actin (Figure 4b). mTOR levels were computed using p-mTOR/t-mTOR densitometry values (Figure 4d). All experiments were performed with at least n (3) biological replicates.

### DISCUSSION

Despite the availability of various treatment options for OSF, the reappearance of fibrotic

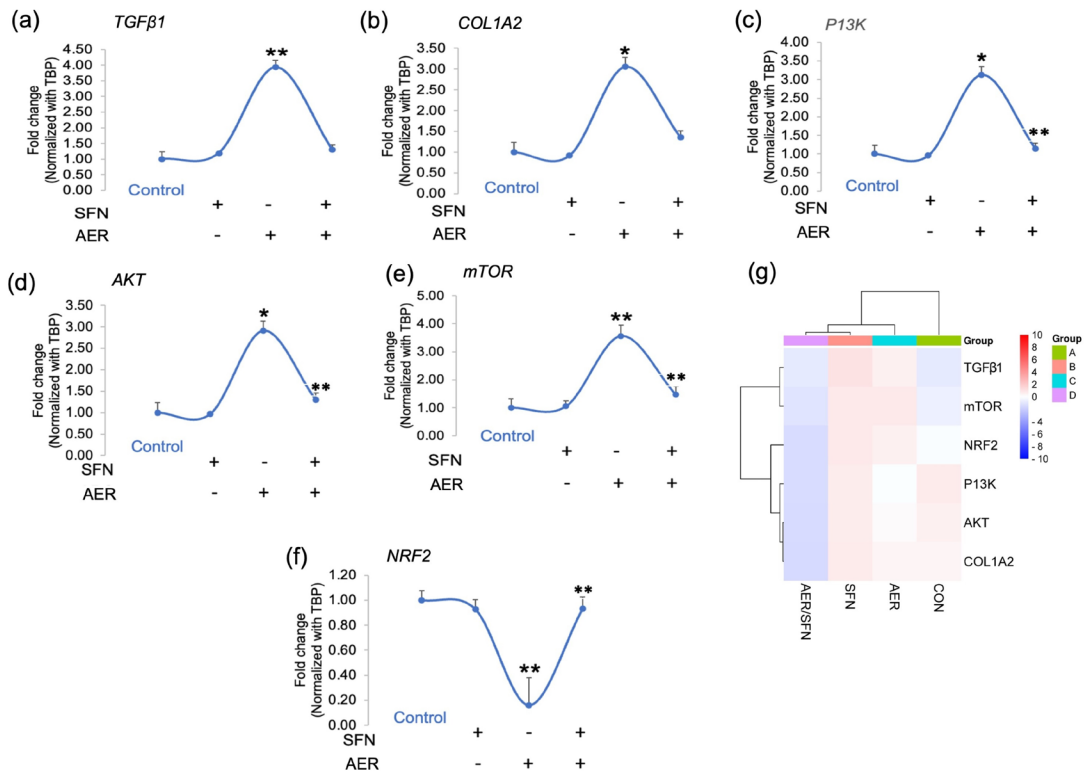


**Figure 3** - Comparative analysis of mRNA expression in HGFs by quantitative polymerase chain reaction assay (a-f) Graphical representation showing a comparison of mRNA expression of TGFβ1, COL1A2, PI3K, AKT-1, mTOR, and NRF2 normalized with TBP. Experimental triplicates were performed. The results were analyzed using a relative quantification (RQ) manager, and CT values were obtained from the percentage of relative expression with normalization using TBP (n=3). Analysis of variance (\*p = <0.05, \*\*p = <0.01) was considered statistically significant. (g) SRplot was used to create the heat map and show the gene cluster orientation of the targeted genes analyzed in this study.

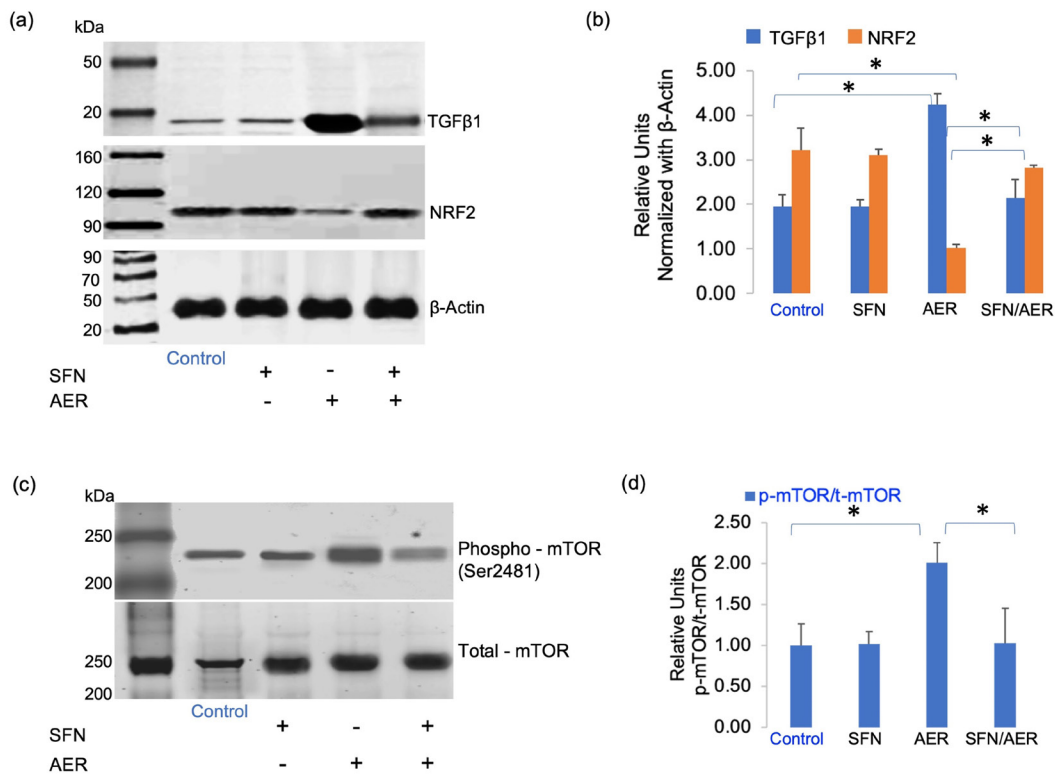


**Figure 4** - Comparative analysis of protein expression in HGFs by western blot assay (a) Protein expression analysis of TGFβ1, NRF2 and β-actin served as the loading control for the respective Control, SFN, AER, SFN/AER; (b) Graphical representation comparing the expression of TGFβ1 and NRF2 normalized with β-actin; (c) Protein expression analysis was conducted for p-mTOR and t-mTOR in the Control, SFN, AER and SFN/AER; (d) The graph illustrates the normalized levels of relative p-mTOR vs t-mTOR (n=3). The analysis of variance showed statistical significance with a p-value (\*p = <0.05).

bands is frequent [30]. Incorporating a potent phytomedicine-based supplementary therapy could improve the predictive results. As reported in studies, SFN is a natural isothiocyanate known for its antibacterial, anti-helminthic, anti-inflammatory, antifibrotic, and antitumorigenic properties. The effectiveness of SFN in combating fibrosis has been investigated in conditions like idiopathic pulmonary fibrosis and liver fibrosis [19,23,31].

In the present study, we demonstrated that treatment with 25  $\mu\text{g}/\text{mL}$  of AER in HGFs significantly upregulated the expression of profibrotic growth factor TGF $\beta$ 1 by 4 folds, which was in correlation to the increase in TGF $\beta$ 1 expression measured by fluorescent intensity quantification. Following this, we observed an upregulation of the downstream target proteins: PI3 by approximately 3.5 folds, AKT by 3 folds, mTOR by 3.5 folds, and COL1A2 by 3 folds ( $p < 0.5^{**}$ ). In addition, on quantitative estimation of soluble collagen, we observed an upregulation of HYP expression to 40 ng/mL compared to the control (20 ng/mL) and SFN-treated group (22 ng/mL). AER is known to induce reactive oxygen species production, TGF $\beta$ 1 activation, and Smad 2 phosphorylation in buccal mucosal fibroblasts (BMFs) [32]. Our results were concurrent with other studies that have also reported a significant upregulation of TGF $\beta$ 1, COL1A2, and COL3A1 in BMFs on treatment with 25  $\mu\text{g}/\text{mL}$  of AER [8,9]. Furthermore, arecanut extract (ANE) has been reported to exhibit a stimulatory effect on collagen 1A1 (COL1A1) and COL3A1 by inhibiting Matrixmetalloproteases 2 and 9 upregulating Tissue inhibitor of Matrixmetalloproteases. The study also demonstrated the inductive effect of ANE on the PI3/AKT/mTOR pathway [33].

The interaction between TGF $\beta$ 1 and the PI3/AKT/mTOR pathway promotes fibrosis. AKT activates downstream mTOR signaling, maintaining low autophagy activity of fibroblasts, thereby preserving the high proliferative and antiapoptotic potential of fibroblasts [12]. The PI3/AKT/mTOR pathway is a master regulator of autophagy; increased fibrosis is linked with defective autophagy, while enhanced autophagy promotes an antifibrotic effect [34]. In the present study, the increase in HYP and COL1A2 expression on AER induction could be attributed to the defective autophagy of the modulated fibroblasts, an outcome of the increased mTOR expression on AER treatment.

On evaluating the other end of the spectrum, treatment with 10  $\mu\text{M}$  of SFN significantly downregulated the expression levels of TGF 1, PI3, AKT, mTOR, COL1A2, and HYP to approximately 1 to 1.5 folds when compared to the AER treated group. Literature evidence states that SFN decreases the catalytic activity of PI3 and AKT (a positive regulator of mTOR), thereby inhibiting mTOR and the consequential excessive deposition of ECM proteins in Human Osteosarcoma (H2OS) cells [20]. Furthermore, to understand the mechanism by which SFN inhibits mTOR, we assessed the effect of SFN on its specific binding protein, NRF2. We observed that SFN treatment significantly upregulated the expression level of the stress response transcription factor NRF2 from 0.2 fold (AER treated) to approximately 1 fold, thereby proposing that SFN inhibits mTOR in the presence of NRF2. Our results were consistent with a study that reported significant attenuation of oxidative stress in mouse models on SFN treatment. This effect was achieved by elevating the expression of antioxidant enzymes such as superoxide dismutase via upregulation of NRF2 expression [23]. On protein analysis, we observed that SFN (10  $\mu\text{M}$ ) treatment in AER-induced HGFs significantly downregulated TGF $\beta$ 1 and relative mTOR (p-mTOR/t-mTOR) expression and upregulated NRF2 expression when compared to the treated group. A study reported that the antifibrotic activity of SFN in attenuating the progression of hepatic fibrosis is through NRF2-mediated inhibition of the TGF $\beta$  signaling pathway, leading to reduced expression of type 1 collagen [19]. Another histopathological study reported that SFN decreases dystrophic muscle fibrosis in mdx mice via NRF2 mediation of TGF $\beta$  signaling, thereby reducing collagen deposition [35]. The above results prove that SFN could significantly alleviate oral fibrosis by inducing autophagy through the PI3/AKT/mTOR pathway via NRF2.

## CONCLUSION

The present in vitro study elucidates the antifibrotic potential of SFN in AER-induced HGFs via NRF2 modulation of the PI3/AKT/mTOR pathway. These results emphasize the importance of exploring non-Smad pathways in the pathogenesis of OSF for targeted intervention. Furthermore, it also demands carrying out in vivo studies on fibrotic models to be able

to develop mechanism based preventive and therapeutic strategies for OSF. Overall, based on the observed results, the authors confirm the research hypothesis.

## ABBREVIATIONS

TGFβ1 – Transforming Growth Factor Beta 1

COL1A2 – Collagen Type 1 Alpha 2

PI3K – Phosphatidylinositol 3 kinase

AKT1 – Serine/Threonine Kinase 1

mTOR – Mammalian Target of Rapamycin

NRF2 – Nuclear Factor Erythroid 2–Related Factor 2

TBP – Tata Box Binding Protein

## Author's Contributions

PNA: Conceptualization, Investigation, Data Curation, Writing – Original Draft Preparation, Writing – Review & Editing. RS: Methodology, Investigation, Data Curation, Writing – Original Draft Preparation, Writing – Review & Editing. RS: Formal Analysis, Writing – Review & Editing. WE: Formal Analysis, Writing – Review & Editing.

## Conflict of Interest

The authors have no conflicts of interest to declare.

## Funding

This research did not receive any specific grant from funding agencies in the public, commercial, or not-for-profit sectors.

## Regulatory Statement

Not-Applicable for this study.

## REFERENCES

1. Rajalalitha P, Vali S. Molecular pathogenesis of oral submucous fibrosis: a collagen metabolic disorder. *J Oral Pathol Med*. 2005;34(6):321-8. <http://doi.org/10.1111/j.1600-0714.2005.00325.x>. PMID:15946178.
2. Muller S, Tilakaratne WM. Update from the 5th edition of the World Health Organization Classification of Head and Neck Tumors: tumours of the oral cavity and mobile tongue. *Head Neck Pathol*. 2022;16(1):54-62. <http://doi.org/10.1007/s12105-021-01402-9>. PMID:35312982.
3. Tilakaratne WM, Ekanayaka RP, Warnakulasuriya S. Oral submucous fibrosis: a historical perspective and a review on

etiology and pathogenesis. *Oral Surg Oral Med Oral Pathol Oral Radiol*. 2016;122(2):178-91. <http://doi.org/10.1016/j.oooo.2016.04.003>. PMID:27422417.

4. Gayathri K, Malathi N, Gayathri V, Adtani PN, Ranganathan K. Molecular pathways of oral submucous fibrosis and its progression to malignancy. *Arch Oral Biol*. 2023;148:105644. <http://doi.org/10.1016/j.archoralbio.2023.105644>. PMID:36804642.
5. Jian X, Jian Y, Wu X, Guo F, Hu Y, Gao X, et al. Oral submucous fibrosis transforming into squamous cell carcinoma: a prospective study over 31 years in mainland China. *Clin Oral Investig*. 2021;25(4):2249-56. <http://doi.org/10.1007/s00784-020-03541-9>. PMID:32844258.
6. Shen YW, Shih YH, Fuh LJ, Shieh TM. Oral submucous fibrosis: a review on biomarkers, pathogenic mechanisms, and treatments. *Int J Mol Sci*. 2020;21(19):7231. <http://doi.org/10.3390/ijms21197231>. PMID:33008091.
7. Warnakulasuriya S, Kujan O, Aguirre-Urizar JM, Bagan JV, Gonzalez-Moles MA, Kerr AR, et al. Oral potentially malignant disorders: a consensus report from an international seminar on nomenclature and classification, convened by the WHO Collaborating Centre for Oral Cancer. *Oral Dis*. 2021;27(8):1862-80. <http://doi.org/10.1111/odi.13704>. PMID:33128420.
8. Adtani PN, Narasimhan M, Punnoose AM, Kambalachenu HR. Antifibrotic effect of *Centella asiatica* Linn and asiatic acid on arecoline-induced fibrosis in human buccal fibroblasts. *J Invest Clin Dent*. 2017;8(2):e12208. <http://doi.org/10.1111/jicd.12208>. PMID:26840561.
9. Adtani P, Malathi N, Ranganathan K, Lokeswari S, Punnoose AM. Antifibrotic effect of *Ocimum basilicum* L. and linalool on arecoline-induced fibrosis in human buccal fibroblasts. *Trans Res Oral Oncol*. 2018;3:1-9. <http://doi.org/10.1177/2057178X18764471>.
10. Lee PH, Chu PM, Hsieh PL, Yang HW, Chueh PJ, Huang YF, et al. Glabridin inhibits the activation of myofibroblasts in human fibrotic buccal mucosal fibroblasts through TGF-beta/smad signaling. *Environ Toxicol*. 2018;33(2):248-55. <http://doi.org/10.1002/tox.22512>. PMID:29119715.
11. Xie H, Jing R, Liao X, Chen H, Xie X, Dai H, et al. Arecoline promotes proliferation and migration of human HepG2 cells through activation of the PI3K/AKT/mTOR pathway. *Hereditas*. 2022;159(1):29. <http://doi.org/10.1186/s41065-022-00241-0>. PMID:35836300.
12. Wang J, Hu K, Cai X, Yang B, He Q, Wang J, et al. Targeting PI3K/AKT signaling for treatment of idiopathic pulmonary fibrosis. *Acta Pharm Sin B*. 2022;12(1):18-32. <http://doi.org/10.1016/j.apsb.2021.07.023>. PMID:35127370.
13. Wang R, Song F, Li S, Wu B, Gu Y, Yuan Y. Salvianolic acid A attenuates CCl(4)-induced liver fibrosis by regulating the PI3K/AKT/mTOR, Bcl-2/Bax and caspase-3/cleaved caspase-3 signaling pathways. *Drug Des Devel Ther*. 2019;13:1889-900. <http://doi.org/10.2147/DDDT.S194787>. PMID:31213776.
14. He J, Peng H, Wang M, Liu Y, Guo X, Wang B, et al. Isoliquiritigenin inhibits TGF-beta1-induced fibrogenesis through activating autophagy via PI3K/AKT/mTOR pathway in MRC-5 cells. *Acta Biochim Biophys Sin*. 2020;52(8):810-20. <http://doi.org/10.1093/abbs/gmaa067>. PMID:32638014.
15. Bendavit G, Aboukassim T, Hilmi K, Shah S, Batist G. Nrf2 transcription factor can directly regulate mTOR: linking cytoprotective gene expression to a major metabolic regulator that generates redox activity. *J Biol Chem*. 2016;291(49):25476-88. <http://doi.org/10.1074/jbc.M116.760249>. PMID:27784786.
16. Ramalingam S, Shantha S, Muralitharan S, Sudhakar U, Thamizhchelvan H, Parvathi VD. Role of tissue markers associated with tumor microenvironment in the progression and immune suppression of oral squamous cell carcinoma. *Med Oncol*. 2023;40(10):303. <http://doi.org/10.1007/s12032-023-02169-5>. PMID:37731058.

17. Arakeri G, Brennan PA. Oral submucous fibrosis: an overview of the aetiology, pathogenesis, classification, and principles of management. *Br J Oral Maxillofac Surg*. 2013;51(7):587-93. <http://doi.org/10.1016/j.bjoms.2012.08.014>. PMID:23107623.
18. Chole RH, Gondivkar SM, Gadbaile AR, Balsaraf S, Chaudhary S, Dhore SV, et al. Review of drug treatment of oral submucous fibrosis. *Oral Oncol*. 2012;48(5):393-8. <http://doi.org/10.1016/j.oraloncology.2011.11.021>. PMID:22206808.
19. Oh CJ, Kim JY, Min AK, Park KG, Harris RA, Kim HJ, et al. Sulforaphane attenuates hepatic fibrosis via NF-E2-related factor 2-mediated inhibition of transforming growth factor-beta/Smad signaling. *Free Radic Biol Med*. 2012;52(3):671-82. <http://doi.org/10.1016/j.freeradbiomed.2011.11.012>. PMID:22155056.
20. Zhang Y, Gilmour A, Ahn YH, de la Vega L, Dinkova-Kostova AT. The isothiocyanate sulforaphane inhibits mTOR in an NRF2-independent manner. *Phytomedicine*. 2021;86:153062. <http://doi.org/10.1016/j.phymed.2019.153062>. PMID:31409554.
21. Tongzhen Xu DR, Sun X, Yang G. Dual roles of sulforaphane in cancer treatment. *Anticancer Agents Med Chem*. 2012;12(9):1132-42. <http://doi.org/10.2174/187152012803529691>. PMID:22583415.
22. Thangapandian S, Ramesh M, Miltonprabu S, Hema T, Jothi GB, Nandhini V. Sulforaphane potentially attenuates arsenic-induced nephrotoxicity via the PI3K/Akt/Nrf2 pathway in albino Wistar rats. *Environ Sci Pollut Res Int*. 2019;26(12):12247-63. <http://doi.org/10.1007/s11356-019-04502-w>. PMID:30835071.
23. Yan B, Ma Z, Shi S, Hu Y, Ma T, Rong G, et al. Sulforaphane prevents bleomycin-induced pulmonary fibrosis in mice by inhibiting oxidative stress via nuclear factor erythroid 2-related factor-2 activation. *Mol Med Rep*. 2017;15(6):4005-14. <http://doi.org/10.3892/mmr.2017.6546>. PMID:28487960.
24. Rao SR, Subbarayan R, Ajitkumar S, Girija DM. 4PBA strongly attenuates endoplasmic reticulum stress, fibrosis and mitochondrial apoptosis markers in cyclosporine treated human gingival fibroblasts. *J Cell Physiol*. 2018;233(1):60-6. <http://doi.org/10.1002/jcp.25836>. PMID:28158898.
25. Mosmann T. Rapid colorimetric assay for cellular growth and survival: application to proliferation and cytotoxicity assays. *J Immunol Methods*. 1983;65(1-2):55-63. [http://doi.org/10.1016/0022-1759\(83\)90303-4](http://doi.org/10.1016/0022-1759(83)90303-4). PMID:6606682.
26. Alley MC, Scudiero DA, Monks A, Hursey ML, Czerwinski MJ, Fine DL, et al. Feasibility of drug screening with panels of human tumor cell lines using a microculture tetrazolium assay. *Cancer Res*. 1988;48(3):589-601. PMID:3335022.
27. Schepici G, Bramanti P, Mazzon E. Efficacy of sulforaphane in neurodegenerative diseases. *Int J Mol Sci*. 2020;21(22):8637. <http://doi.org/10.3390/ijms21228637>. PMID:33207780.
28. Dieffenbach C, Lowe T, Dveksler G. General concepts for PCR primer design. *PCR Methods Appl*. 1993;3(3):S30-7. <http://doi.org/10.1101/gr.3.3.S30>. PMID:8118394.
29. Adtani P, Narasimhan M, Ranganathan K, Punnoose A, Prasad P, Natarajan P. Characterization of oral fibroblasts: an in vitro model for oral fibrosis. *J Oral Maxillofac Pathol*. 2019;23(2):198-202. [http://doi.org/10.4103/jomfp.JOMFP\\_28\\_19](http://doi.org/10.4103/jomfp.JOMFP_28_19). PMID:31516223.
30. Gupta SJM, Jawanda MK. Oral submucous fibrosis: an overview of a challenging entity. *Indian J Dermatol Venereol Leprol*. 2021;87(6):768-77. [http://doi.org/10.25259/IJDVL\\_371\\_20](http://doi.org/10.25259/IJDVL_371_20). PMID:33969655.
31. Kyung SY, Kim DY, Yoon JY, Son ES, Kim YJ, Park JW, et al. Sulforaphane attenuates pulmonary fibrosis by inhibiting the epithelial-mesenchymal transition. *BMC Pharmacol Toxicol*. 2018;19(1):13. <http://doi.org/10.1186/s40360-018-0204-7>. PMID:29609658.
32. Hsieh YP, Wu KJ, Chen HM, Deng YT. Arecoline activates latent transforming growth factor beta1 via mitochondrial reactive oxygen species in buccal fibroblasts: suppression by epigallocatechin-3-gallate. *J Formos Med Assoc*. 2018;117(6):527-34. <http://doi.org/10.1016/j.jfma.2017.07.003>. PMID:28720506.
33. Dai JP, Chen XX, Zhu DX, Wan QY, Chen C, Wang GF, et al. Panax notoginseng saponins inhibit areca nut extract-induced oral submucous fibrosis in vitro. *J Oral Pathol Med*. 2014;43(6):464-70. <http://doi.org/10.1111/jop.12158>. PMID:24484214.
34. Peng J, Xiao X, Li S, Lyu X, Gong H, Tan S, et al. Aspirin alleviates pulmonary fibrosis through PI3K/AKT/mTOR-mediated autophagy pathway. *Exp Gerontol*. 2023;172:112085. <http://doi.org/10.1016/j.exger.2023.112085>. PMID:36623738.
35. Sun C, Li S, Li D. Sulforaphane mitigates muscle fibrosis in mdx mice via Nrf2-mediated inhibition of TGF-beta/Smad signaling. *J Appl Physiol*. 2016;120(4):377-90. <http://doi.org/10.1152/jappphysiol.00721.2015>. PMID:26494449.

**Pooja Narain Adtani**

**(Corresponding address)**

Gulf Medical University, College of Dentistry, Department of Basic Medical and Dental Sciences, Ajman, United Arab Emirates.

Email: dr.pooja@gmu.ac.ae

Date submitted: 2023 Dec 01

Accepted submission: 2024 Mar 14